Polyfluorinated Bis-styrylbenzene β-Amyloid Plaque Binding Ligands

Daniel P. Flaherty,[†] Shannon M. Walsh,[‡] Tomomi Kiyota,[‡] Yuxiang Dong,[†] Tsuneya Ikezu,[‡] and Jonathan L. Vennerstrom*,[†]

University of Nebraska Medical Center, College of Pharmacy, 986025 Nebraska Medical Center, Omaha, Nebraska 68198, and University of Nebraska Medical Center, College of Medicine, 985880 Nebraska Medical Center, Omaha, Nebraska 68198

Received January 22, 2007

β-Amyloid (Aβ) binding affinities and specificities for six bis-styrylbenzenes with multiple magnetically equivalent fluorine atoms in the form of a tetrafluorophenyl core or symmetrical trifluoromethyl and trifluoromethoxy groups were determined by means of fluorescence titrations with amyloid peptide $A\beta_{1-40}$ and a novel in vitro fluorescence-based assay using APP/PS1 transgenic mouse brain sections. Bis-styrylbenzenes with a tetrafluorophenyl core had increased Aβ binding affinities compared to their monofluorophenyl or phenyl counterparts. Bis-styrylbenzenes with carboxylic acid functional groups had lower Aβ binding affinities than their neutral counterparts. Selected bis-styrylbenzenes were demonstrated to have good blood−brain barrier penetration capabilities. These data extend the SAR of bis-styrylbenzene Aβ binding and provide direction for the development of a noninvasive probe for early detection of Alzheimer's disease using ^{19}F MRI.

Introduction

Alzheimer's disease (AD),[1] a relatively common neurodegenerative disorder in the elderly,[2,3] is characterized by an accumulation of senile plaques containing aggregated protein deposits of amyloid (Aβ) fibrils, numerous neurofibrillary tangles (NFTs), reactive astrocytes, and activated microglia in the neocortex and hippocampus.[4,5] Senile plaques can contain either a diffuse amyloid deposition (presumably early senile plaques) or a dense core of insoluble Aβ with neuritic structures (mature senile plaques). Although Aβ deposition and NFTs are commonly observed in nondemented elderly, 80 years and older, increased levels of senile plaques are seen in AD brains.[6,7] The degree of both Aβ deposition and NFT formation are correlated with cognitive decline.[6,8−10] The molecular pathogenesis of AD is centered on Aβ production and its clearance. Aβ is generated by the processing of amyloid precursor protein (APP) by processing enzymes, and is cleared from the brain by its diffusion, export to vascular system, phagocytosis, or degradation. The amyloid cascade hypothesis[11] for AD pathogenesis proposes that accumulation and aggregation of the Aβ triggers a cascade that leads to the characteristic pathologies of AD. The strongest support for this hypothesis comes from genetic studies of familial AD. These studies reveal that Aβ accumulation or aggregation is elevated by mutations of the APP, PS1, and PS2 genes directly related to Aβ production and other risk factors (apoE).[12] Therefore, it would be beneficial to identify Aβ-binding ligands with high specificity and sensitivity that could be used for early in vivo detection of AD and for monitoring the progression of the disease.

The discovery of the fluorescent Aβ-binding diazo dye Congo red[13] provided the starting point for the synthesis of numerous compounds with potential as in vivo imaging agents using positron emission tomography (PET), single photon emission computed tomography (SPECT), and magnetic resonance imaging (MRI). The diazo disalicylate Chrysamine G[14] was one of the first Congo red derivatives to be investigated as a candidate for PET and SPECT imaging. This soon led to the synthesis of a number of bis-styrylbenzenes with strong Aβ plaque binding. These include **1** (X-34),[15] **2** (FSB),[16] **3** (BSB),[17,18] **4** (IMSB),[19,20] and **5** (K114).[21] Importantly, intravenously administered **2** or **3** can cross the blood−brain barrier (BBB) and bind to Aβ plaques deposited in APP or APP/PS1 mice.[16,17,22] Early data suggested that interactions between cationic amino acid residues of the Aβ peptide with the sulfonic acid functional groups of Congo red and the carboxylic acid functional groups of Chrysamine G and **1**−**3** were necessary for Aβ-ligand binding.[14] However, as illustrated by **5**, acidic functional groups are not necessarily required for good Aβ binding.[21]

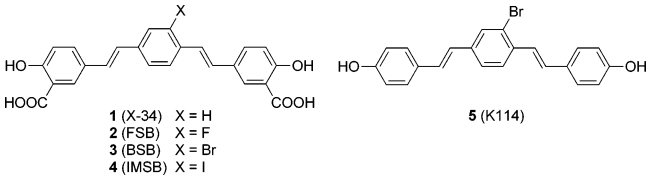

1 (X-34) X = H
2 (FSB) X = F
3 (BSB) X = Br
4 (IMSB) X = I

5 (K114)

Design. Monofluoro bis-styrylbenzene **2**[16] has been proposed as a potential in vivo probe for Aβ plaques using ^{19}F MRI.[22] To address the low ^{19}F MRI sensitivity inherent in the structure of **2**, we designed bis-styrylbenzene ligands with multiple magnetically equivalent fluorine atoms in the form of a tetrafluorophenyl core (**6**−**8**) or symmetrical trifluoromethyl (**9**, **10**) and trifluoromethoxy (**11**, **12**) groups (Schemes 1 and 2). FSB (**2**) and the nonfluorinated bis-styrylbenzene **13** served as controls. For each of these, Aβ binding affinity and specificity were determined. We also assessed the potential of selected bis-styrylbenzenes (**8**, **11**, **14**) to penetrate the BBB. These data that we present in this paper extend the SAR of bis-styrylbenzene Aβ binding and provide direction for the development of a noninvasive probe for AD using ^{19}F MRI.

Chemistry. Bis-styrylbenzene **2** was obtained using the procedure of Sato et al.[16] with two modifications. First, the dimethylation of 5-formylsalicylic acid to afford **16** was achieved in 78% yield using dimethyl sulfate rather than methyl iodide (65% yield). Second, the key 1-fluoro-2,5-bis(bromomethyl)benzene intermediate was obtained in a one-step benzylic bromination of 3-fluoro-4-methylbenzyl bromide (49% yield) using *N*-bromosuccinimide (NBS)/2,2′-azobis(isobutyronitrile)

* To whom correspondence should be addressed. Tel.: 402-559-5362. Fax: 402-559-9543. E-mail: jvenners@unmc.edu.
[†] College of Pharmacy.
[‡] College of Medicine.

10.1021/jm070085f CCC: $37.00
Published on Web 09/11/2007

Scheme 1. Synthesis of Bis-styrylbenzenes **6**−**8**

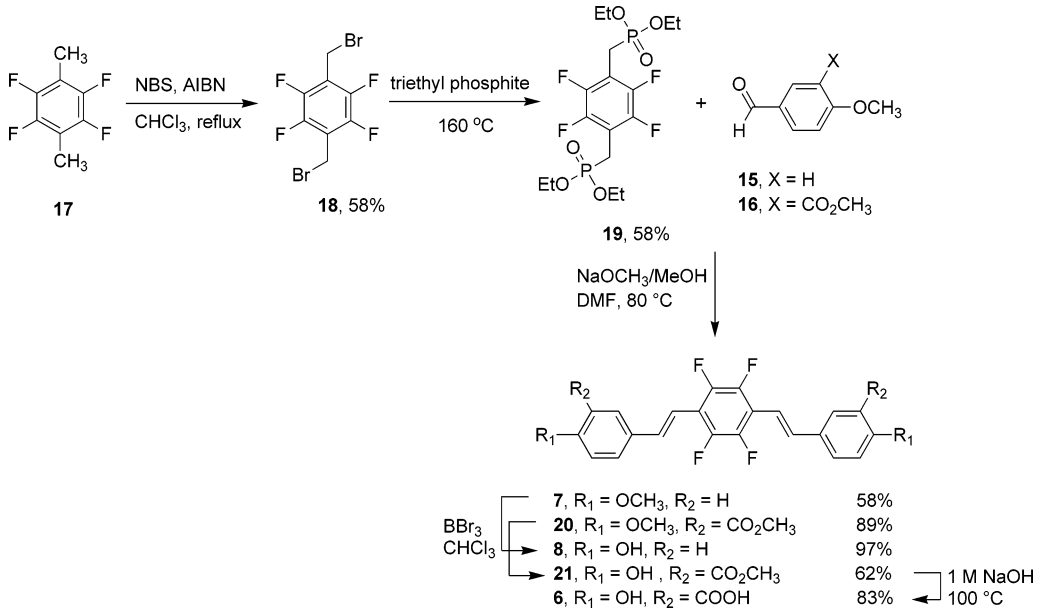

Scheme 2. Synthesis of Bis-styrylbenzenes **9**−**14**

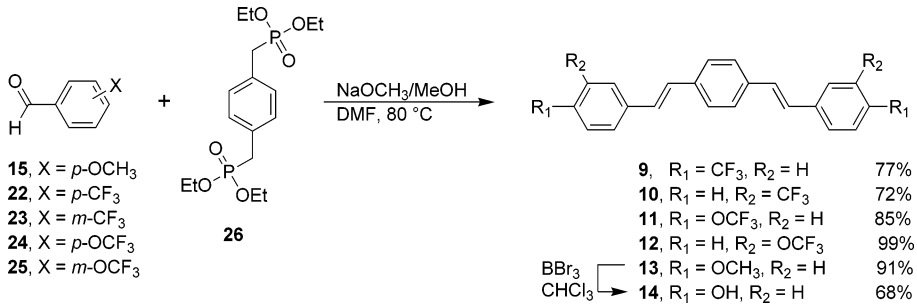

(AIBN) rather than the low yielding (6% overall) two-step procedure starting with 2-fluoro-*p*-xylene using diazonium chemistry.[16]

As illustrated in Schemes 1 and 2, bis-styrylbenzenes **7**, **9**−**13**, and **20** were obtained in yields of 58−91% using classic Wittig (Horner−Wadsworth−Emmons) couplings between benzaldehydes and the ylides derived from bisdiethylphosphonates. Bis-styrylbenzene **13**[23] has also been obtained using Heck chemistry.[24] Phenolic bis-styrylbenzenes **8** (97%), **14** (68%), and **21** (62%) were obtained by subsequent boron tribromide demethylation. Finally, bis-styrylbenzene **6** was obtained in 83% yield by ester hydrolysis of **21**. As expected, clean singlets were obtained in the ^{19}F NMR spectra of target polyfluorinated bis-styrylbenzenes **6**−**12**.

***β*-Amyloid (A*β*) Binding Affinity and Specificity.** *β*-Amyloid (A*β*) binding affinity and specificity for bis-styrylbenzenes **6**, **8**−**12**, and **14**, with bis-styrylbenzene **2** and thioflavin T as controls, was determined by means of fluorescence titrations[25] with amyloid peptide Aβ_{1-40} and a novel in vitro fluorescence-based assay using APP/PS1 transgenic mouse brain sections. We could not obtain data for **6** and **13** due to their low solubility in phosphate buffered saline (PBS)/ethanol cosolvent mixtures. The APP/PS1 transgenic mice were developed by crossing the Tg2576 strain,[26] which express the K670N/M671L mutant of APP695 found as Swedish familial AD gene, and the M146L 6.1 strain,[27] which express the M146L mutant of PS1 found as the early onset familial AD gene. By measuring the fluorescent intensities of A*β* plaques (specific signal) and background regions (noise; Figure 1) using the same fluorescence image capturing setting,[28] we were able to calculate a signal/noise (S/N) ratio, a measure of A*β* binding specificity. This A*β* binding specificity represents the relative affinity of a compound for A*β* plaques compared to normal brain tissue.

In considering the A*β* binding affinity (K_d) and specificity (S/N ratio) data (Table 1), we note that the K_d of 560 nM that we obtained for thioflavin T was quite similar to the value (K_d = 750 nM) reported by Lockhart et al.[25] Although varying amounts of ethanol were required to solubilize the bis-styrylbenzenes (9:1 PBS/ethanol for **2**, **6**, and **14** and 2:3 PBS/ethanol for **8**−**12**), the proportion of ethanol had little effect on the measured binding affinities. For example, the K_d (nM) values in 9:1 versus 2:3 PBS/ethanol for **2** were 3400 ± 200 versus 3300 ± 100 and for **6** were 9.4 ± 0.8 versus 6.4 ± 0.4.

The FSB control (**2**) had the weakest binding affinity of all of the bis-styrylbenzenes, although it did have high specificity, exceeded only by that of **14**. The binding affinity for tetrafluorophenyl bis-styrylbenzene **6** increased 360-fold compared to its monofluorophenyl counterpart **2**, albeit with a 4-fold loss in specificity. Similarly, the binding affinity of **8**, with its tetrafluorophenyl core, was 370-fold greater than **14**, its phenyl counterpart; this was accompanied by a 2-fold lower specificity. As revealed by the ^{13}C NMR signals for the central aromatic carbon atoms of **8** (144.0 ppm) and **14** (126.5 ppm),[29] the more electropositive tetrafluorophenyl core in **6** and **8** apparently provides a stronger interaction with A*β* compared to the corresponding monofluorophenyl (**2**) or phenyl (**14**) cores. In addition, the multiple fluorine atoms of **6** and **8** can form hydrogen bonds and interact with cations,[30] both of which could

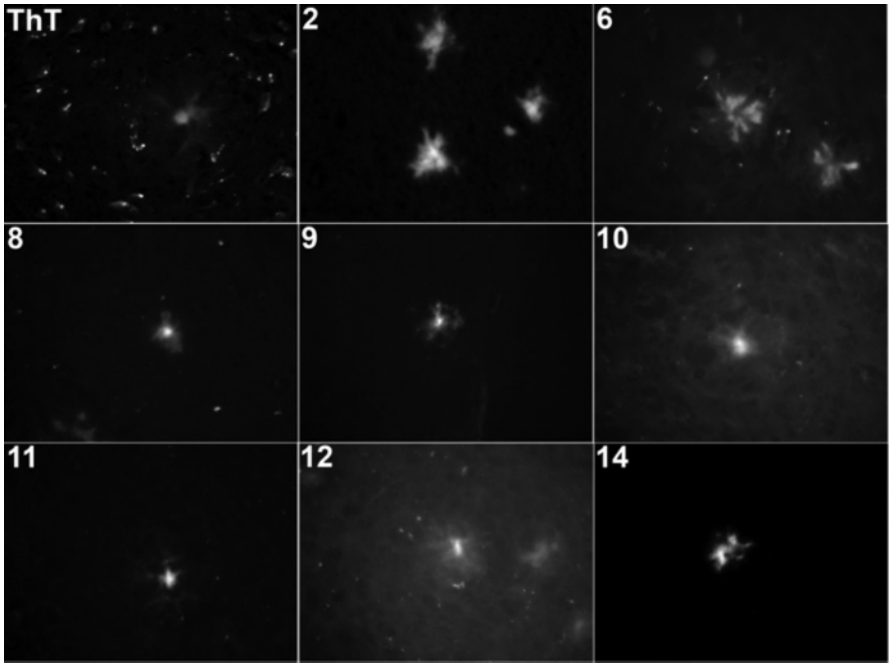

Figure 1. Fluorescence imaging of Aβ plaque in aged APP/PS1 mouse brain. Frozen brain sections (10 μm thickness) were stained with 50 μM of each compound for 8 min in 1:1 PBS/ethanol, washed successively with 75% aq ethanol, 95% aq ethanol, and xylene. Fluorescence images were taken using a Nikon TE-2000, 40× Pan Fluor objective, and Roper HQ CCD camera (400× original magnification). Ex/Em wavelengths are 488/520 (FITC filter set) for thioflavin T (ThT), and 360/460 (DAPI filter set) for **2**, **6**, **8**−**12**, and **14**. Original magnification: 400×.

Table 1. Amyloid Peptide $A\beta_{1-40}$ Binding Affinity (K_d) and Aβ Plaque Binding Specificity (S/N Ratio) to APP/PS1 Transgenic Mouse Brain Slices for Thioflavin T and Bis-styrylbenzenes **2**, **6**, **8**−**12**, and **14**

cmpd	K_d[a] (nM)	S/N ratio[b]
thioflavin T	560 ± 20	6.1 ± 0.5
2	3400 ± 200	14 ± 0.8
6	9.4 ± 0.8	3.6 ± 0.2
8	0.030 ± 0.001	10 ± 1.3
9	9.5 ± 0.3	8.5 ± 0.5
10	26 ± 1	10 ± 1.3
11	10 ± 1	8.6 ± 0.2
12	16 ± 1	7.8 ± 1.3
14	11 ± 2	17 ± 1.3

[a] Values represent the average ± SD of three determinations. [b] Values represent the average ± SD of five determinations.

contribute to the higher binding affinities of **6** compared to **2** and of **8** compared to **14**. The superior binding affinity and specificity for the neutral **8** versus the acidic **6** is consistent with previous data,[21] suggesting that acidic functional groups are not required for good Aβ binding. The data for **11** versus **14** indicate that phenol functional groups are also not required for good Aβ binding. The data for **9** versus **10** and **11** versus **12** suggest that *para*- is marginally superior to *meta*-substitution on the outer phenyl rings.

While the binding specificity data (Table 1) obtained from the APP/PS1 transgenic mouse brain sections (Figure 1) were useful, this model did not permit us to differentiate compound binding to sheet structures other than Aβ such as NFTs. To this end, we stained human AD brain sections containing both Aβ senile plaques and NFTs (Figure 2) with **2**, **8**, **11**, and **14**. These data show that **8** (D, E) and **11** (G, H) stain mostly Aβ plaques, **14** (J, K) stains both Aβ plaques and NFTs, and **2** (A, B) rather preferentially stains NFTs. There was no specific staining by any of the compounds in age-matched control brain sections (C, F, I, L), demonstrating the binding specificity of these bis-styrylbenzenes for AD sheet structures. The preferential staining of **2** to NFTs is consistent with its low binding affinity for Aβ (Table 1).

In Vivo BBB Delivery of Bis-styrylbenzenes into Aβ Plaque-Bearing APP/PS1 Mouse Brain. We next determined whether intravenously administered **8**, **11**, and **14** (with **2** as a control) could cross the BBB and bind to Aβ plaque. Bis-styrylbenzenes **2**, **8**, **14** (10 mg/kg), or **11** (5 mg/kg) were injected (100 μL total volume) into 11-month-old APP/PS1 mice through the tail vein. The 10 mg/kg dose was based on previous investigations.[17,22,31,32] For **11**, the highest dose possible was 5 mg/kg, as its solubility was 10-fold lower than the other bis-styrylbenzenes. The animals were sacrificed at 48 h after injection, and the frozen brain sections were stained with hematoxylin for histology. As shown in Figure 3, all of the bis-styrylbenzenes crossed the BBB and bound to Aβ plaques in vivo. APP/PS1 mice brain sections treated with **14** (A, B, E, F), **2** (C, D, G, H), **8** (I, J, M, N), and **11** (K, L, O, P) each showed intense Aβ plaque signals. Each fluorescent signal is Aβ plaque-specific as determined by hematoxylin counterstaining (see arrows in the matched fluorescent and histology images: A and E, B and F, C and G, D and H, etc.). Control nontransgenic animals showed no specific signals in the brain for any of the tested compounds after intravenous injection (data not shown). These data confirm that these bis-styrylbenzene derivatives retain the BBB penetration capabilities of **2** and that **8** and **11** have the potential for Aβ detection using ^{19}F MRI. MRI experiments with **8** and **11** are ongoing and will be reported in due course.

Summary. These data extend the SAR of bis-styrylbenzene Aβ binding and provide direction for the development of a noninvasive probe for early detection of AD using ^{19}F MRI. Although **14**, one of the nonfluorinated bis-styrylbenzene control compounds, is obviously not a candidate for a ^{19}F MRI AD imaging probe, its structure provides a core skeleton for the discovery of additional polyfluorinated derivatives.

Experimental Section

General. Starting materials were purchased from Aldrich, TCI, Acros, Avocado, or Apollo Scientific. All reactions were run under a positive pressure of Ar. Melting points were determined on a

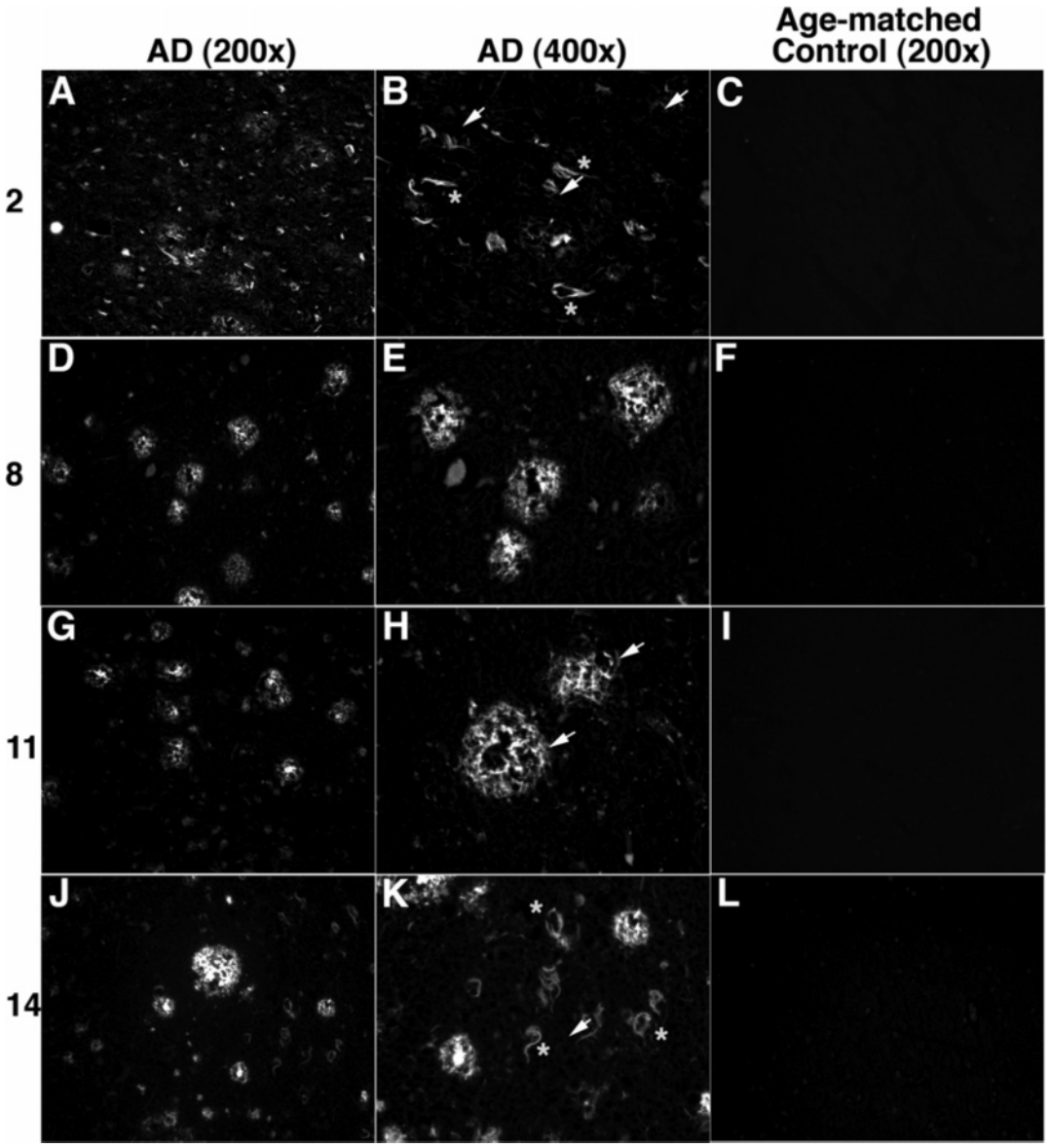

Figure 2. Fluorescence staining of AD and control brain sections by **2**, **8**, **11**, or **14**. Paraffin sections (7 μm thickness) of AD cortex (left and middle columns) and age-matched control cortex (right column) were deparaffinized, chemically bleached for autofluorescence, and stained with 10 μM of **2** (A-C), **8** (D−F), **11** (G-I), or **14** (J-L). Arrows indicate representative Aβ plaques, and * denotes representative neurofibrillary tangles (B, E, H, K). Original magnifications: 200× (left and right columns) and 400× (middle column).

Mel-Temp apparatus and are uncorrected. ^{1}H (500 MHz), ^{13}C (125.7 MHz), and ^{19}F (470 MHz) NMR spectra were measured on a Varian spectrometer using $CDCl_3$ and DMSO-d_6 as solvents. All chemical shifts are reported in parts per million (ppm) and are relative to internal $(CH_3)_4Si$ for ^{1}H, $CDCl_3$ (77.0 ppm) and DMSO-d_6 (39.7 ppm) for ^{13}C NMR, and $C_6H_5CF_3$ (−63.72 ppm) for ^{19}F NMR. Microanalyses were performed by M-H-W Laboratories, Phoenix, AZ.

(*E*,*E*)-1,2,4,5-Tetrafluoro-3,6-bis(3-hydroxycarbonyl-4-hydroxy)styrylbenzene (6). To (*E*,*E*)-1,2,4,5-tetrafluoro-3,6-bis(3-methoxycarbonyl-4-hydroxy)styrylbenzene (**21**; 0.105 g, 0.209 mmol) was added 1.0 M NaOH (0.126 g, 3.14 mL, 3.14 mmol) and the solution was stirred at 100 °C for 5.5 h. After cooling to rt, the solution was quenched with 5 mL of water and 1 mL of 6.0 M HCl to afford, after filtering and drying, **6** (0.082 g, 83%): mp 329−332 °C dec. ^{1}H NMR (DMSO-d_6) 6.71 (d, J = 8.3 Hz, 2H), 6.85 (d, J = 16.6 Hz, 2H), 7.38 (d, J = 16.6 Hz, 2H), 7.56 (d, J = 8.3 Hz, 2H), 7.92 (d, J = 2.4 Hz, 2H). ^{13}C NMR (DMSO-d_6) 109.1, 114.5 (brs), 117.3, 119.2, 124.6, 129.2, 131.2, 137.4, 144.0 (d, J = 240 Hz), 165.0, 171.1. ^{19}F NMR ($C_6H_5CF_3$) −147.87 (s, 4F). Anal. ($C_{24}H_{14}F_4O_6 \cdot 7/6H_2O$) C, H; H: calcd, 3.32; found, 2.89.

General Procedure for the Horner−Wadsworth−Emmons Reactions. (*E*,*E*)-1,2,4,5-Tetrafluoro-3,6-bis(4-methoxy)styrylbenzene (7). A 30 wt % solution of sodium methoxide in methanol (0.260, 0.87 mL, 4.62 mmol) was added to a stirred mixture of 1,2,4,5-tetrafluoro-3,6-bis(diethylphosphonylmethyl)benzene (**19**; 1.040 g, 2.31 mmol) and *p*-anisaldehyde (**15**; 0.705 g, 4.62 mmol) in DMF (10 mL) at rt. This mixture was then heated to 80 °C for 2 h. The reaction was then quenched with 2:1 DMF/H_2O (15 mL), and the precipitate was filtered and rinsed with DMF and ether affording **7** (0.556 g, 58%): mp 197−200 °C. ^{1}H NMR ($CDCl_3$) 3.85 (s, 6H), 6.93 (d, J = 8.8 Hz, 5H), 6.97 (s, 1H), 7.46 (d, J = 16.6 Hz, 2H), 7.50 (d, J = 8.3 Hz, 4H). ^{13}C NMR ($CDCl_3$) 55.4, 111.9, 114.3, 114.8 (brs), 128.3, 129.7, 136.3, 144.6 (brd, J = 259.6 Hz), 160.2. ^{19}F NMR ($C_6H_5CF_3$) −146.14 (s, 4F). Anal. ($C_{24}H_{18}F_4O_2$) C, H.

(*E*,*E*)-1,2,4,5-Tetrafluoro-3,6-bis(4-hydroxy)styrylbenzene (8). A 1.0 M solution of boron tribromide in dichloromethane (0.924 g, 3.69 mL, 3.69 mmol) was added dropwise over 10 min to a stirred suspension of **7** (0.255 g, 0.62 mmol) in chloroform (10 mL) at rt. The reaction mixture was stirred for an additional 2 h at rt before quenching with ∼25 mL of water to afford **8** (0.206 g, 97%) as a precipitate, which was filtered, washed with water and ethyl acetate, and dried: mp 275−277 °C dec. ^{1}H NMR (DMSO-

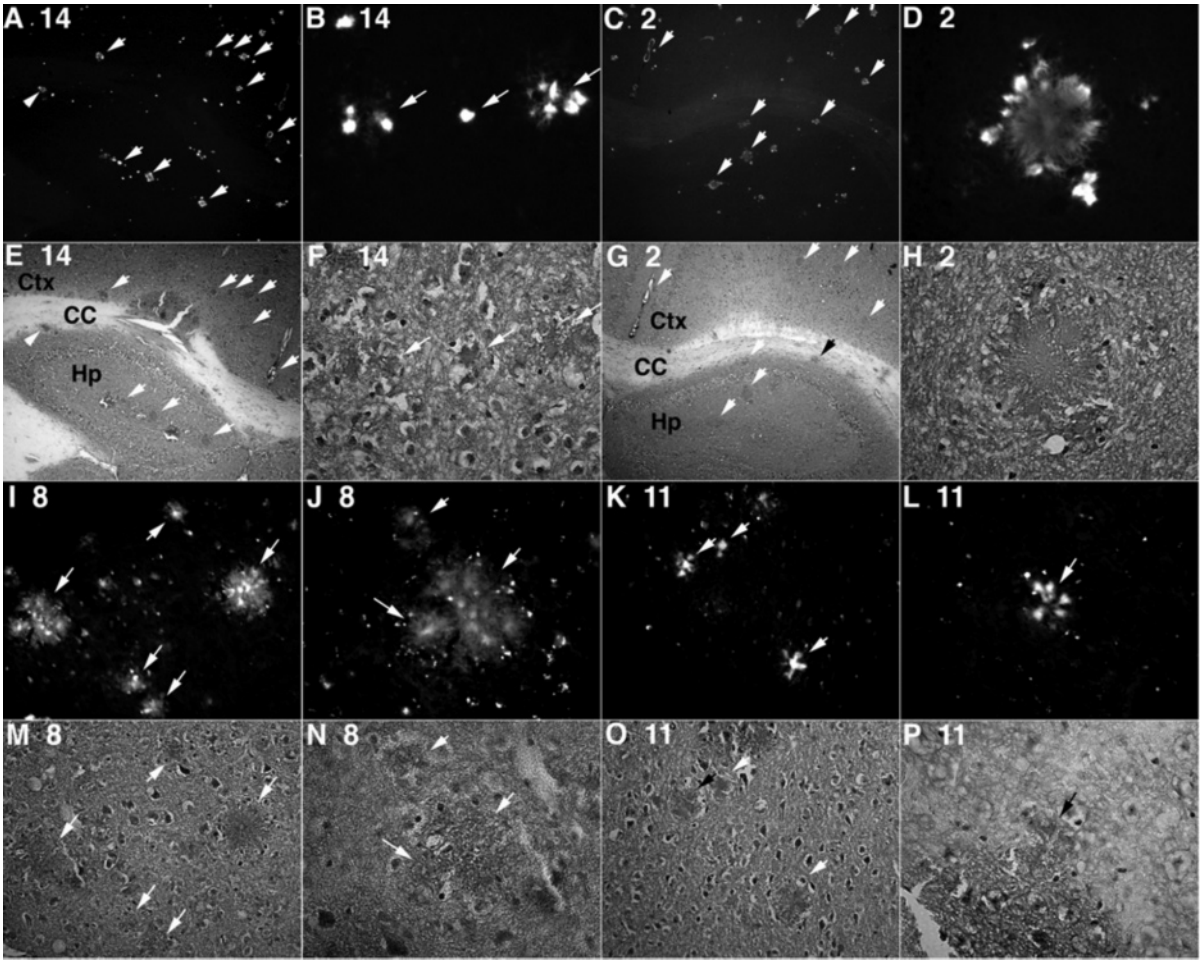

Figure 3. In vivo labeling of Aβ plaques via intravenous injection of **2**, **8**, **11**, or **14** in aged APP/PS1 mice. Eleven-month-old APP/PS1 mice were injected with 10 mg/kg of **2**, **8**, **11**, or **14** in 100 μL volumes via the tail vein and sacrificed at 48 h after injection. Fixed frozen sections (10 μm thickness) were hematoxylin stained, and both fluorescence and histological images were captured using 4× (A, C, E, G), 20× (I, K, M, O), or 40× (B, D, F, H, J, L, N, P) objectives on a Nikon TE-300 with CCD camera. Arrows indicate colocalization of fluorescence-labeled Aβ deposition and hematoxylin staining in cortex (Ctx), corpus callosum (CC), or hippocampus (Hp; A, C, E, G). High-power magnification images (20× and 40×) show representative fluorescent staining of Aβ plaques by **2**, **8**, **11**, or **14**.

d_6) 6.81 (d, J = 8.3 Hz, 4H), 6.91 (d, J = 16.6 Hz, 2H), 7.38 (d, J = 16.6 Hz, 2H), 7.52 (d, J = 7.8 Hz, 4H). ^{13}C NMR (DMSO-d_6) 110.1, 114.6 (brs), 116.0, 127.4, 128.9, 137.2, 144.0 (ddd, J = 249.6, 22.1, 5.7 Hz), 158.8. ^{19}F NMR ($C_6H_5CF_3$) −145.7 (s, 4F). Anal. ($C_{22}H_{14}F_4O_2$) C, H.

(*E*,*E*)-1,4-Bis(4-trifluoromethyl)styrylbenzene (9). Compound **9** was prepared as described above from 1,4-bis(diethylphosphonylmethyl)benzene (**26**; 0.706 g, 1.87 mmol) and 4-trifluoromethylbenzaldehyde (**22**; 0.65 g, 3.74 mmol) to afford **9** (0.593 g, 77%): mp 272−275 °C. ^{1}H NMR ($CDCl_3$) 7.15 (d, J = 16.6 Hz, 2H), 7.20 (d, J = 16.6, 2H), 7.55 (s, 4H), 7.62 (s, 8H). ^{13}C NMR ($CDCl_3$) 124.2 (q, J = 282.2 Hz), 126.7 (q, J = 3.8 Hz), 126.6, 127.2, 127.4, 129.4 (q, J = 31.67 Hz), 130.6, 136.6, 140.7. ^{19}F NMR ($C_6H_5CF_3$) −63.46 (s, 6F). Anal. ($C_{24}H_{16}F_6$) C, H.

(*E*,*E*)-1,4-Bis(3-trifluoromethyl)styrylbenzene (10). Compound **10** was prepared as described above from **26** (0.700 g, 1.85 mmol) and 3-trifluoromethylbenzaldehyde (**23**; 0.645 g, 3.7 mmol) to afford **10** (0.56 g, 72%): mp 138−140 °C. ^{1}H NMR ($CDCl_3$) 7.15 (d, J = 17.0 Hz, 2H), 7.19 (d, J = 17.0 Hz, 2H), 7.48 (t, J = 7.3 Hz, 2H), 7.52 (d, J = 11.5 Hz, 2H), 7.55 (s, 4H), 7.69 (d, J = 7.8, 2H), 7.77 (s, 2H). ^{13}C NMR ($CDCl_3$) 122.0 (q, J = 285.2 Hz), 123.1 (q, J = 3.8 Hz), 124.1 (q, J = 3.4 Hz), 125.2, 127.1, 127.3, 129.2, 129.6, 129.9, 131.2 (q, J = 32.1 Hz), 136.6, 138.0. ^{19}F NMR ($C_6H_5CF_3$) −63.77 (s, 6F). Anal. ($C_{24}H_{16}F_6$) C, H.

(*E*,*E*)-1,4-Bis(4-trifluoromethoxy)styrylbenzene (11). Compound **11** was prepared as described above from **26** (0.50 g, 1.32 mmol) and 4-trifluoromethoxybenzaldehyde (**24**; 0.506 g, 2.64 mmol) to yield **11** (0.47 g, 85%): mp 235−238 °C. ^{1}H NMR ($CDCl_3$) 7.07 (d, J = 13.0 Hz, 2H), 7.11 (d, J = 19.6 Hz, 2H), 7.21 (d, J = 8.3 Hz, 4H), 7.52 (s, 4H), 7.53 (d, J = 8.8 Hz, 4H). ^{13}C NMR ($CDCl_3$) 120.5 (q, J = 257.2 Hz), 121.2, 127.0, 127.2, 127.7, 129.2, 136.0, 136.6, 148.5. ^{19}F NMR ($C_6H_5CF_3$) −58.81 (s, 6F). Anal. ($C_{24}H_{16}F_6O_2$) C, H.

(*E*,*E*)-1,4-Bis(3-trifluoromethoxy)styrylbenzene (12). Compound **12** was prepared as described above from **26** (0.50 g, 1.32 mmol) and 3-trifluoromethoxybenzaldehyde (**25**; 0.506 g, 2.64 mmol) to yield **12** (0.55 g, 99%): mp 168−170 °C. ^{1}H NMR ($CDCl_3$) 7.11 (d, J = 13 Hz, 2H), 7.13 (d, J = 11.2 Hz, 2H), 7.15 (d, J = 15.0 Hz, 2H), 7.38 (s, 2H), 7.40 (t, J = 8.3 Hz, 2H), 7.46 (d, J = 11.2 Hz, 2H), 7.55 (s, 4H). ^{13}C NMR ($CDCl_3$) 118.7, 119.9, 120.5 (q, J = 257.2 Hz), 124.9, 127.1, 127.3, 129.8, 130.0, 136.5, 139.4, 149.7. ^{19}F NMR ($C_6H_5CF_3$) −58.65 (s, 6F). Anal. ($C_{24}H_{16}F_6O_2$) C, H.

(*E*,*E*)-1,4-Bis(4-methoxy)styrylbenzene (13).[23,24] Compound **13** was prepared (as described for **7)** from **26** (0.701 g, 1.85 mmol) and *p*-anisaldehyde (**15**; 0.505 g, 3.70 mmol) to afford **13** (0.58 g, 91%): mp 303−305 °C (lit.[23] mp 310−311 °C). ^{1}H NMR ($CDCl_3$) 3.84 (s, 6H), 6.91 (d, J = 8.8 Hz, 4H), 6.97 (d, J = 16.1 Hz, 2H), 7.08 (d, J = 16.1 Hz, 2H), 7.46 (d, J = 8.8 Hz, 4H), 7.47 (s, 4H).

(*E*,*E*)-1,4-Bis(4-hydroxy)styrylbenzene (14).[24] A 1.0 M solution of boron tribromide in dichloromethane (2.19 g, 8.73 mL, 8.73 mmol) was added dropwise to **13** (0.498 g, 1.45 mmol) in chloroform (20 mL) at 0 °C. The reaction proceeded for 1 h and was quenched with ∼30 mL of water to form a precipitate that was filtered and identified as **14** (0.31 g, 68%): mp 310−312 °C dec (lit.[23] mp 360 °C). ^{1}H NMR (DMSO-d_6) 6.77 (d, J = 8.3 Hz,

4H), 7.00 (d, $J = 16.6$ Hz, 2H), 7.15 (d, $J = 16.6$ Hz, 2H), 7.43 (d, $J = 8.8$ Hz, 4H), 7.52 (s, 4H), 9.57 (s, 2H). ^{13}C NMR (DMSO-d_6) 115.8, 125.0, 126.5, 128.0, 128.2, 128.3, 136.5, 157.6.

3-Methoxycarbonyl-4-methoxybenzaldehyde (16).[16] 5-Formylsalicylic acid (1.47 g, 8.82 mmol) was dissolved in acetone (125 mL) with stirring. Dimethyl sulfate (2.780 g, 22.05 mmol) and potassium carbonate (2.67 g, 19.5 mmol) were added, and the reaction was stirred at reflux for 5.5 h. The solid potassium sulfate was filtered and the solvent was removed in vacuo to give a solid crude product that was crystallized in two crops from ethanol to afford **16** (1.343 g, 78%): mp 83−85 °C. ^{1}H NMR (DMSO-d_6) 3.83 (s, 3H), 3.94 (s, 3H), 7.38 (d, $J = 8.8$ Hz, 1H), 8.09 (dd, $J = 8.8$ Hz, 2.4, 1H), 8.20 (d, $J = 2.4$ Hz, 1H), 9.92 (s, 1H). ^{13}C NMR ($CDCl_3$) 52.3, 56.5, 112.3, 120.6, 129.1, 134.4, 134.5, 163.6, 165.5, 190.0.

1,2,4,5-Tetrafluoro-3,6-bis(bromomethyl)benzene (18).[33] To a stirred solution of 2,3,5,6-tetrafluoro-*p*-xylene (**17**; 4.90 g, 0.0275 mol) in $CHCl_3$ (300 mL) at rt was added NBS (16.08 g, 0.0903 mol) and 2′2′-azobis(isobutyronitrile) (0.23 g, 1.4 mmol). The reaction mixture was heated to reflux for 15 h. The cooled reaction mixture was then washed with H_2O (2 × 300 mL) and dried with $MgSO_4$. After removal of the $CHCl_3$ solvent in vacuo, the residue was crystallized from ethanol to afford **18** (5.34 g, 58%): mp 88−90 °C (lit.[33] mp 125−126 °C). ^{1}H NMR ($CDCl_3$) 4.51 (s, 4H).

1,2,4,5-Tetrafluoro-3,6-bis(diethylphosphonylmethyl)benzene (19).[33] A mixture of triethyl phosphite (5.212 g, 3.14 mmol) and **18** (5.266 g, 15.7 mmol) were heated to 160 °C for 4 h. The solid residue was crystallized from ethyl ether to afford **19** (4.079 g, 58%): mp 73−75 °C (lit.[33] mp 41−42 °C). ^{1}H NMR ($CDCl_3$) 1.30 (t, $J = 6.8$ Hz, 12H), 3.26 (d, $J = 20.5$ Hz, 4H), 4.06−4.18 (m, 8H).

(*E*,*E*)-1,2,4,5-Tetrafluoro-3,6-bis(3-methoxycarbonyl-4-methoxy)styrylbenzene (20). Compound **20** was prepared as described above from **16** (0.748 g, 3.85 mmol) and **19** (0.867 g, 1.93 mmol) to yield **20** (0.91 g, 89%): mp 251−253 °C. ^{1}H NMR ($CDCl_3$) 3.94 (s, 6H), 3.95 (s, 6H), 7.00 (d, $J = 17.1$ Hz, 2H), 7.01 (d, $J = 8.8$ Hz, 2H), 7.46 (d, $J = 16.6$ Hz, 2H), 7.66 (dd, $J = 8.8$ Hz, 2.4 Hz, 2H), 7.99 (d, $J = 2.4$ Hz, 2H). ^{13}C NMR ($CDCl_3$) 52.2, 56.2, 112.4, 113.1, 114.9 (brs), 120.5, 129.1, 130.3, 131.8, 135.4, 144.6 (d, $J = 237.0$ Hz), 159.5, 166.4. ^{19}F NMR ($C_6H_5CF_3$) −145.63 (s, 4F). Anal. ($C_{28}H_{22}F_4O_6$) C, H.

(*E*,*E*)-1,2,4,5-Tetrafluoro-3,6-bis(3-methoxycarbonyl-4-hydroxy)styrylbenzene (21). To a stirred suspension of **20** (0.510 g, 0.961 mmol) in chloroform (34 mL) was added a 1.0 M solution of boron tribomide in methylene chloride (1.45 g, 5.77 mmol) at 0 °C. The reaction mixture was stirred for 10 min, warmed to rt, and stirred for an additional 1 h before quenching with water (30 mL) to form a yellow precipitate. Filtration and washing with water and ethyl acetate afforded **21** (0.299 g, 62%): mp 265−267 °C. ^{1}H NMR ($CDCl_3$) 4.08 (s, 6H), 6.99 (d, $J = 33.7$ Hz, 2H), 7.02 (d, $J = 25.4$ Hz, 2H), 7.44 (d, $J = 16.6$ Hz, 2H), 7.71 (dd, $J = 8.3$ Hz, 2.4 Hz, 2H), 8.00 (d, $J = 2.0$ Hz, 2H). ^{13}C NMR—too insoluble to generate data. ^{19}F NMR ($C_6H_5CF_3$) −145.72 (s, 4F). Anal. ($C_{26}H_{18}F_4O_6$) C, H.

1-Fluoro-2,5-bis(bromomethyl)benzene.[16] 3-Fluoro-4-methylbenzyl bromide (3.00 g, 14.8 mmol) and NBS (2.89 g, 16.2 mmol) in chlorform (300 mL) were heated to reflux at which time 2′2-azobis(isobutyronitrile) (0.036 g, 0.22 mmol) was added. The reaction mixture was refluxed for 10 h, cooled, and washed with water. The chloroform layer was dried with $MgSO_4$ and filtered, and the solvent was removed in vacuo to afford an off-white solid that was crystallized from ethanol (15 mL) to afford 1-fluoro-2,5-bis(bromomethyl)benzene (1.79 g, 42%): mp 322−325 °C dec (lit.[16] mp 294 °C dec). ^{1}H NMR ($CDCl_3$) 4.43 (s, 2H), 4.49 (s, 2H), 7.12 (dd, $J = 10.3$, 1.5 Hz), 7.15 (dd, $J = 7.8$, 1.5 Hz), 7.37 (t, $J = 7.3$ Hz).

In Vitro Aβ_{1-40} Binding Affinity Determination by Fluorescence Titration. Amyloid (Aβ) binding affinities (K_d) for **6**, **8**−**12**, and **14**, with **2** and thioflavin T as controls, were determined by means of fluorescence titrations,[25] with amyloid peptide Aβ_{1-40} at 23 °C. Intrinsic fluorescence intensity (FLINT) changes associated with ligand binding to aggregated Aβ_{1-40} were recorded on a Cary Eclipse fluorescence spectrophotometer (Varian) using excitation wavelengths determined for each compound. Fixed concentrations of Aβ_{1-40} (500 nM for thioflavin T and **2**; 40 nM for **14**; 25 nM for **9**−**12**; 10 nM for **6**; 1 nM for **8**) were diluted to 500 μL in 9:1 (thioflavin T and **14**) or 2:3 (**2**, **6**, **8**−**12**) PBS/ethanol in a 10 mm quartz fluorescence cuvette. With the exception of **8**, concentrations of Aβ_{1-40} were selected to be no more than 10-fold higher than compound binding affinities to obtain accurate K_d values. This indicates that the measured K_d for **8** is a minimum value, and the true binding affinity may be higher. To the Aβ_{1-40} PBS/ethanol solution in the cuvette, aliquots of test compounds in PBS/ethanol were titrated using a 2.0 μL Hamilton syringe with a reproducibility adapter along a concentration gradient of compound (0.8 nM—saturation). Fluorescence spectra were recorded until the fluorescence no longer increased with increasing compound concentration (saturation). The FLINT at these wavelengths were plotted versus compound concentrations to yield binding isotherms. Compound Aβ_{1-40} K_d values were determined (Prism 4.0c software, GraphPad, Inc.) by means of the standard thermodynamic relationship for single-site ligand/receptor binding: $B = K(L)/1 + K(L)$.

In Vitro Aβ Plaque Binding Specificity Using APP/PS1 Transgenic Mouse Brain Slices. Thioflavin T, **2**, **6**, **8**−**12**, and **14** were dissolved in chloroform or DMSO at 25 mM, diluted to 0.50 mM with ethanol and then diluted with 1:1 PBS/ethanol to prepare a solution of 50 μM. The fluorescence spectra of **6**, **8**−**12**, and **14** were determined to obtain peak excitation and emission wavelengths (Ex/Em nm) to select the fluorescence filter/dichroic mirror settings of the microscope (Nikon TE-2000U). Eleven-month-old transgenic APP/PS1 mice derived from crossing Tg2576 expressing APP Swedish mutant and M146L 6.1 line expressing presenilin-1 mutant[26,27] were anesthetized and transcardically perfused with 4% paraformaldehyde in PBS under the guidance of Institutional Animal Care and Use Committee. The fixed brain samples were cryoprotected in 20% sucrose in PBS and subjected to cryostat sectioning (Leica). Frozen brain sections (10 μm thickness) of aged APP/PS1 transgenic mice (three sections per dilution point) were stained with the compound solutions for 30 min, and then washed successively with 75% aq ethanol, 95% aq ethanol, and xylene. Fluorescence imaging of the stained and washed brain sections were carried out using a DAPI filter (Chroma) and a Roper HQ CCD camera (original magnification: 400×) following a standard BSB/FSB staining protocol.[18,22] Fluorescence images of one plaque per section were systematically captured using the same image acquisition setting (laser power, capturing time, photomultiplier setting) to obtain comparable fluorescent intensities of five plaque regions (specific signal) and five background regions (noise signal) to obtain signal-to-noise (S/N) ratios.

Fluorescence Staining of AD and Control Brain Sections by 2, 8, 11, or 14. Paraffin sections (7 μm thickness) of AD cortex and age-matched control cortex were deparaffinized before incubation with 3% $KMnO_4$ for 4 min according to the autofluorescence chemical bleaching method of Sun et al.[34] The slides were then rinsed with water, treated with a solution of 1% $K_2S_2O_5$ and 1% oxalic acid until the brown color faded, washed again with water, treated with freshly prepared 1% $NaBH_4$ in water for 5 min, and washed three times with water and PBS. The slides were then stained with 10 μM of **2**, **8**, **11**, and **14** as described in the previous section.

In Vivo BBB Delivery of 2, 8, 11, or 14 into Aβ Plaque-Bearing APP/PS1 Mouse Brain. Eleven-month-old APP/PS1 mice were injected with 10 mg/kg of **2**, **8**, **11**, or **14** in 100 μL volumes of PBS with 10% DMSO via the tail vein and sacrificed at 48 h after injection by transcardial perfusion of 4% paraformaldehyde in PBS. After cryoprotection and cryosectioning, fixed frozen brain sections (10 μm thickness) were hematoxylin stained, and both fluorescence and histological images were captured with a Nikon TE-300 Magnafire CCD camera using a DAPI filter for fluorescence. The fluorescent images depict the in vivo labeling of Aβ plaques by the intravenously injected **2**, **8**, **11**, or **14**.

Acknowledgment. This investigation received financial support from the Vada Oldfield Alzheimer Research Foundation (T.I.), the National Institute of Health (P01NS043985; T.I.), and the Department of Pharmaceutical Sciences, College of Pharmacy, University of Nebraska Medical Center (J.L.V.). We thank K. Ashe and K. Duff for providing Tg2576 and PS1M146L mice, J. Buescher for transgenic mouse colony maintenance and genotyping, Paul A. Keifer and Edward L. Ezell for assistance with NMR experiments, and Tessa Smolik and Amanda Mausbach for synthesis of intermediates.

Supporting Information Available: Elemental analysis data for **6**−**12**, **20**, and **21**, the proton decoupled ^{13}C NMR spectra of **8** and **14**, HMBC and HSQC spectra of **14**, the fluorescence properties of **2**, **6**, **8**−**12**, and **14**, and representative Aβ_{1-40} binding isotherms for thioflavin T and **8**. This material is available free of charge via the Internet at http://pubs.acs.org.

References

(1) Goedert, M.; Spillantini, G. A Century of Alzheimer's Disease. *Science* **2006**, *314*, 777−781.
(2) Hebert, L. E.; Scherr, P. A.; Bienias, J. L.; Bennett, D. A.; Evans, D. A. Alzheimer Disease in the U.S. Population: Prevalence Estimates Using the 2000 Census. *Arch. Neurol*. **2003**, *60*, 1119−1122.
(3) Brookmeyer, R.; Gray, S.; Kawas, C. Projections of Alzheimer's Disease in the United States and the Public Health Impact of Delaying Disease Onset. *Am. J. Public Health* **1998**, *88*, 1337−1342.
(4) Alzheimer, A. Ueber eine eigenartige Erkrankung der Hirnrinde. *Allg. Z. Psychiatr*. **1907**, *64*, 146−148.
(5) Selkoe, D. J. Alzheimer's Disease: Genotypes, Phenotypes, and Treatments. *Science* **1997**, *275*, 630−631.
(6) Berg, L.; McKeel, D. W., Jr.; Miller, J. P.; Baty, J.; Morris, J. C. Neuropathological Indexes of Alzheimer's Disease in Demented and Nondemented Persons Aged 80 Years and Older. *Arch. Neurol.* **1993**, *50*, 349−358.
(7) Schmitt, F. A.; Davis, D. G.; Wekstein, D. R.; Smith, C. D.; Ashford, J. W.; Markesbery, W. R. "Preclinical" AD Revisited: Neuropathology of Cognitively Normal Older Adults. *Neurology*. **2000**, *55*, 370−376.
(8) Wilcock, G. K.; Esiri, M. M. Plaques, Tangles and Dementia. A Quantitative Study. *J. Neurol. Sci*. **1982**, *56*, 343−356.
(9) Braak, H.; Braak, E. Staging of Alzheimer's Disease-Related Neurofibrillary Changes. *Neurobiol. Aging* **1995**, *16*, 271−284.
(10) Naslund, J.; Haroutunian, V.; Mohs, R.; Davis, K. L.; Davies, P.; Greengard, P.; Buxbaum, J. D. Correlation Between Elevated Levels of Amyloid Beta-peptide in the Brain and Cognitive Decline. *JAMA, J. Am. Med. Assoc*. **2000**, *283*, 1571−1577.
(11) Hardy, J.; Selkoe, D. J. The Amyloid Hypothesis of Alzheimer's Disease: Progress and Problems on the Road to Therapeutics. *Science* **2002**, *297*, 353−356.
(12) Strittmatter, W. J; Saunders, A. M.; Schmechel, D; Pericak-Vance, M.; Enghild, J.; Salvesen, G. S.; Roses, A. D. Apolipoprotein E: High-Avidity Binding to Amyloid and Increased Frequency of Type 4 Allele in Late-Onset Familial Alzheimer Disease. *Proc. Natl. Acad. Sci. U.S.A.* ***1993***, *90*, 1977−1981.
(13) Puchtler, H.; Sweat, F.; Levine, M. On the Binding of Congo Red by Amyloid. *J. Histochem. Cytochem.* **1962**, *10*, 355−364.
(14) Klunk, W. E.; Debnath, M. L.; Pettegrew, J. W. Chrysamine-G binding to Alzheimer and Control Brain: Autopsy Study of a New Amyloid Probe. *Neurobiol. Aging* **1995**, *16*, 541−548.
(15) Styren, S. D.; Hamilton, R. L.; Styren, G. C.; Klunk, W. E. X-34, a Fluorescent Derivative of Congo Red: A Novel Histochemical Stain for Alzheimer's Disease Pathology. *J. Histochem. Cytochem.* **2000**, *48*, 1223−1232.
(16) Sato, K.; Higuchi, M.; Iwata, N.; Saido, T. C.; Sasamoto, K. Fluoro-Substituted and ^{13}C-Labeled Styrylbenzene Derivatives for Detecting Brain Amyloid Plaques. *Eur. J. Med. Chem.* **2004**, *39*, 573−578.
(17) Skovronsky, D. M.; Zhang, B.; Kung, M. P.; Kung, H. F.; Trojanowski, J. Q.; Lee, V. M. Y. In Vivo Detection of Amyloid Plaques in a Mouse Model of Alzheimer's Disease. *Proc. Natl. Acad. Sci. U.S.A.* **2000**, *97*, 7609−7614.
(18) Schmidt, M. L.; Schuck, T.; Sheridan, S.; Kung, M. P.; Kung, H.; Zhuang, Z. P.; Bergeron, C.; Lamarche, J. S.; Skovronsky, D.; Giasson, B. I.; Lee, V. M.; Trojanowski, J. Q. The Fluorescent Congo Red Derivative, (*trans*,*trans*)-1-Bromo-2,5-bis-(3-hydroxycarbonyl-4-hydroxy)styrylbenzene (BSB), Labels Diverse Beta-Pleated Sheet Structures in Postmortem Human Neurodegenerative Disease Brains. *Am. J. Pathol.* **2001**, *159*, 937−943.
(19) Kung, M. P.; Hou, C.; Zhuang, Z. P.; Skovronsky, D. M.; Zhang, B.; Gur, T. L.; Trojanowski, J. Q.; Lee, V. M.; Kung, H. F. Radioiodinated Styrylbenzene Derivatives as Potential SPECT Imaging Agents for Amyloid Plaque Detection in Alzheimer's Disease. *J. Mol. Neurosci.* **2002**, *19*, 7−10.
(20) Zhuang, Z. P.; Kung, M. P.; Skovronsky, D. M.; Gur, T. L.; Plössl, K.; Trojanowski, J. Q.; Lee, V. M.-Y.; Kung, H. F. Radioiodinated Styrylbenzenes and Thioflavins as Probes for Amyloid Aggregates. *J. Med. Chem.* **2001**, *44*, 1905−1914.
(21) Crystal, A. S.; Giasson, B. I.; Crowe, A.; Kung, M. P.; Zhuang, Z. P.; Trojanowski, J. Q.; Lee, V. M. Y. A Comparison of Amyloid Fibrollogenesis using the Novel Fluorescent Compound K114. *J. Neurochem.* **2003**, *86*, 1359−1368.
(22) Higuchi, M.; Iwata, N.; Matsuba, Y.; Sato, K.; Sasamoto, K.; Saido, T. C. ^{19}F and ^{1}H MRI Detection of Amyloid Beta Plaques In Vivo. *Nat. Neurosci*. **2005**, *8*, 527−533.
(23) Tewari, R.; Kumari, N.; Kendurkar, P. Studies on Ylides: Stereospecific Synthesis of *trans*,*trans*-Distyrylbenzenes and *trans*,*trans*-Divinylbenzenes. *Indian J. Chem., Sect B: Org. Chem. Incl. Med. Chem.* **1977**, *15*, 753−755.
(24) Bayly, S. R.; Humphrey, E. R.; de Chair, H.; Paredes, C. G.; Bell, Z. R.; Jeffery, J. C.; McCleverty, J. A.; Ward, M. D.; Totti, F.; Gatteschi, D.; Courric, S.; Steele, B. R.; Screttas, C. G. Electronic and Magnetic Metal-Metal Interactions in Dinuclear Oxomolybdenum(V) Complexes Across *bis*-Phenolate Bridging Ligands with Different Spacers Between the Phenolate Termini: Ligand-Centered vs Metal-Centered Redox Activity. *J. Chem. Soc., Dalton Trans*. **2001**, *9*, 1401−1414.
(25) Lockhart, A.; Ye, L.; Judd, D. B.; Merritt, A. T.; Lowe, P. N.; Morgenstern, J. L.; Hong, G.; Gee, A. D.; Brown, J. Evidence for the Presence of Three Distinct Binding Sites for the Thioflavin T Class of Alzheimer's Disease PET Imaging Agents on Amyloid Peptide Fibrils. *J. Biol. Chem.* **2005**, *280*, 7677−7684.
(26) Hsiao, K.; Chapman, P.; Nilsen, S.; Eckman, C.; Harigaya, Y.; Younkin, S.; Yang, F.; Cole, G. Correlative Memory Deficits, Abeta Elevation, and Amyloid Plaques in Transgenic Mice. *Science* **1996**, *274*, 99−102.
(27) Duff, K.; Eckman, C.; Zehr, C.; Yu, X.; Prada, C. M.; Perez-tur, J.; Hutton, M.; Buee, L.; Harigaya, Y.; Yager, D.; Morgan, D.; Gordon, M. N.; Holcomb, L.; Refolo, L.; Zenk, B.; Hardy, J.; Younkin, S. Increased Amyloid-beta42(43) in Brains of Mice Expressing Mutant Presenilin 1. *Nature* **1996**, *383*, 710−713.
(28) The S/N ratio is independent of a target compound's fluorescence Ex/Em and extinction coefficient (ϵ_{ex}; see Supporting Information). This is illustrated by the complete lack of correlation ($r = -0.045$, $P = 0.90$) between ϵ_{ex} and S/N ratio for the compounds in Table 1.
(29) Peak assigment from HSQC and HMBC experiments (see Supporting Information).
(30) Razgulin, A. V.; Mecozzi, S. Binding Properties of Aromatic Carbon-Bound Fluorine. *J. Med. Chem*. **2006**, *49*, 7902−7906.
(31) Hoefert, V. B; Aiken, J. M.; McKenzie, D.; Johnson, C. J. Labeling of the Scrapie-Associated Prion Protein In Vitro and In Vivo. *Neurosci. Lett.* **2004**, *371*, 176−180.
(32) Ishikawa, K.; Doh-ura, K.; Kudo, Y.; Nishida, N.; Murakami-Kubo, I.; Ando, Y.; Sawada, T.; Iwaki, T. Amyloid Imaging Probes are Useful for Detection of Prion Plaques and Treatment of Transmissible Spongiform Encephalopathies. *J. Gen. Virol.* **2004**, *85*, 1785−1790.
(33) Krebs, F. C.; Jensen, T. Fluorinated Molecules Relevant to Conducting Polymer Research. *J. Fluorine Chem.* **2003**, *120*, 77−84.
(34) Sun, A.; Nguyen, X. V.; Bing, G. Comparative Analysis of an Improved Thioflavin-S Stain, Gallyas Silver Stain, and Immunohistochemistry for Neurofibrillary Tangle Demonstration on the Same Sections. *J. Histochem. Cytochem.* **2002**, *50*, 463−472.

JM070085F